Jurnal Teknologi

Full Paper

INTEGRATING RVS AND DCR FOR A COMPREHENSIVE SEISMIC VULNERABILITY ASSESSMENT OF EXISTING BUILDINGS

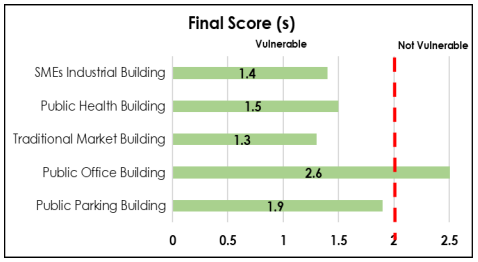
Indar Trimulyani Minatin[a,c], Yenny Nurchasanah[b]*, Mochamad Solikin[b]

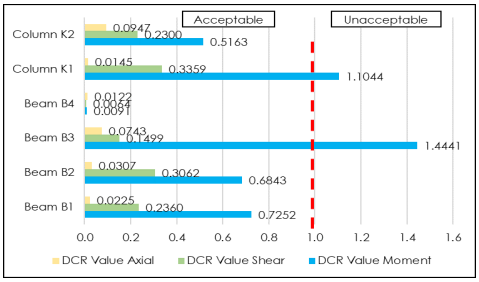
[a]Faculty of Civil Engineering Study Program, Universitas Muhammadiyah Surakarta, Indonesia
[b]Civil Engineering Study Program, Engineering Faculty, Universitas Muhammadiyah Surakarta, Indonesia
[c]Civil Engineering Study Program, Engineering Faculty, Universitas Muhammadiyah Luwuk, Central Sulawesi, Indonesia

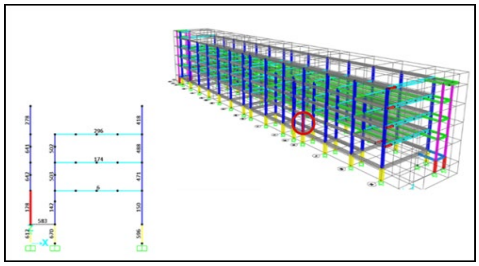
Article history
Received
14th September 2025
Received in revised form
11th February 2026
Accepted
27th February 2026
Published
1st November 2026

*Corresponding author
yn205@ums.ac.id

Graphical abstract







Abstract

Southeast Asia faces significant seismic risk, but many public buildings in developing countries still lack adequate vulnerability assessments to address earthquake hazards. This study evaluated the vulnerability of buildings by integrating the Rapid Visual Screening (RVS) and Demand Capacity Ratio (DCR) methods at five government-owned public buildings in Surakarta, Central Java. The RVS analysis showed that four of five buildings had scores < 2, indicating high earthquake vulnerability. Furthermore, the DCR assessment revealed inconsistencies in public parking buildings and health facilities with respect to the strong-column-weak-beam principle as stipulated in SNI 1726:2019. Key factors affecting vulnerability include building irregularities, soil types, and regulatory standards during the planning process. The integration of RVS and DCR provides a more comprehensive evaluation process by combining a quick visual inspection with an in-depth structural capacity analysis. This study offers a practical contribution by providing a tool for relevant authorities to identify and prioritize strengthening building structures to reduce the impact of future seismic disasters.

***Keywords*:** Earthquake, Seismic vulnerability, Rapid Visual Screening, Demand Capacity Ratio, Building.

©2026 Penerbit UTM Press. All rights reserved

DOI: https://doi.org/10.11113/jurnalteknologi.v88.25549

1.0 INTRODUCTION

Southeast Asia is a region with very high seismic activity, so it often experiences earthquakes that are difficult to predict accurately and can cause significant infrastructure damage and fatalities [1],[2],[3]. Globally, Indonesia ranks second in Southeast Asia in disaster risk [4], particularly for seismic hazards. This occurs due to its geographical position at the convergence zone of the Eurasian, Indo-Australian, and Pacific tectonic plates [5],[6], which drives continuous tectonic deformation through subduction and active faulting. This vulnerability is clearly illustrated by major earthquakes recorded in Indonesia, such as the 2004 Aceh earthquake [7], the 2006 Yogyakarta-Central Java earthquake [8], the 2018 Palu earthquake [9], and the 2018 Lombok earthquake[10].

Recent findings on tectonic plate convergence in the southern region indicate that the city of Surakarta, Central Java Province, has been classified as a high-seismic-risk zone (red zone) in Central Java [11],[12]. This condition is evidenced by a recent magnitude 5.3 earthquake with an epicenter near Surakarta, approximately 142 km away [13]. The high seismic risk level in Surakarta is influenced not only by regional earthquake sources but also by local soil conditions that tend to amplify ground shaking. These soil characteristics are similar to those found in the Klaten area, which experienced the most severe damage during the 2006 Yogyakarta earthquake due to soil amplification effects [11]. Furthermore, Surakarta is one of the most densely populated cities in Central Java [14], thereby increasing the potential for infrastructure damage, particularly to buildings, which may directly increase the risk of casualties and significant social and economic losses.

Earthquakes can occur repeatedly due to the accumulation of tectonic stress along active faults that are constantly subjected to pressure from the movement of the Earth's plates [15],[16],[17]. To prepare for future earthquakes, appropriate mitigation measures are needed to reduce the negative impacts they may cause [18], [19], [20].

The Rapid Visual Screening (RVS) and Demand Capacity Ratio (DCR) methods are generally used separately in assessing the vulnerability of buildings to earthquakes. FEMA 154-based RVS is effective as a fast, economical, visually based initial screening stage, but it cannot quantitatively represent structural performance [21] In contrast, the DCR method can technically evaluate the resilience of structures by comparing earthquake forces with structural element capacities [22], but, according to FEMA 310, its application requires an initial screening process [23].

This study proposes an integrated Rapid Visual Screening (RVS) and Demand Capacity Ratio (DCR) framework that advances seismic vulnerability assessment beyond stand-alone visual classification. In this approach, RVS functions as an initial filter to identify buildings requiring further evaluation, which is then validated through structural capacity analysis using DCR. Compared to probabilistic methods such as fragility functions that rely on extensive empirical data and complex modeling, the integrated RVS–DCR approach offers a more practical and efficient alternative for assessing existing buildings in earthquake-prone areas with limited data and inspection time. By combining rapid screening with targeted quantitative verification, this framework improves the reliability of vulnerability classification and provides a rational basis for prioritizing mitigation strategies and supporting informed decision-making in seismic risk management [24],[25].

2.0 METHODOLOGY

2.1 Research Approach

This study employs a quantitative approach to objectively measure and analyze the seismic vulnerability of buildings. Numerical data and technical parameters are collected using Rapid Visual Screening (RVS) and Demand Capacity Ratio (DCR) methods, which generate scores and ratios for statistical analysis. The study also evaluates structural performance in accordance with SNI 1726:2019, using calculations and mathematical modelling to assess structures' capacity to resist seismic loads.

2.2 Population and sample

This research focuses on low- to medium-rise buildings in the city of Surakarta. Five buildings were selected as research samples; their selection was based on their function as public buildings that provide public services. This selection is based on the consideration that earthquake damage to the building can significantly affect the social, economic, and sustainable aspects of city activities. Building data is collected directly from relevant government agencies. The selected buildings include a public parking building, a public office building, a traditional market building, a public health building, and an SMEs (small and medium enterprises) industrial building.

2.3 Tools

This study used the FEMA 154 vulnerability assessment form for Rapid Visual Screening (RVS) analysis and FEMA 356 for Demand Capacity Ratio (DCR) analysis. Structural element analysis was conducted using SAP2000 version 22 software, with all calculations based on SNI 1726:2019, the latest regulation for earthquake-resistant buildings in Indonesia.

DOI: https://doi.org/10.11113/jurnalteknologi.v88.25549

2.4 Assessment of existing building vulnerability using Rapid Visual Screening (RVS)

Assessing building vulnerability with the Rapid Visual Screening (RVS) method requires following FEMA 154 guidelines. Key procedures for identifying vulnerability using RVS are outlined below [26].

Field observation is conducted to ensure the completeness of existing data on the buildings in the study, specifically those that are already standing and still in operation.

The determination of seismicity zones at the research location was conducted as a reference for selecting the RVS form. In this study, the determination of seismicity zones at the site utilized https://rsa.ciptakarya.pu.go.id/, ensuring that the identified seismicity zones align with the actual seismic conditions.

The selection of RVS forms involves this process to ensure that the forms used are appropriate for the seismic conditions at the research site, thereby making the building vulnerability results more accurate and representative.

The field survey and completion of the RVS form involved direct inspection of the selected buildings, followed by completing the form to obtain the basic and modifier score values. The basic score was determined by identifying the building type and structural system, while the modifier score was obtained by evaluating vertical and plan irregularities, construction year, and local soil type [27],[28]. These parameters directly impact the seismic vulnerability assessment, as each influences the scores recorded in the RVS form, helping to accurately identify building vulnerabilities [29].

The final RVS score is calculated once all forms have been completed. This score is the primary indicator of a building's vulnerability to earthquakes and is calculated using the formula in Equation (1) [26].

$$\text{Final Score} = \text{Basic Score} + \text{Modifiers Score} \quad (1)$$

A final score greater than 2 indicates that the building is safe, and no further assessment is needed. If the score is 2 or less, the building is classified as high risk and requires additional structural evaluation analysis [26].

After obtaining the final score, the next step is to calculate the probability building collapse. This calculation estimates the probability of collapse during a major earthquake, based on the final score derived from the previous assessment. The probability of building collapse is determined using Equation (2) [26].

$$\text{Probability Building Collapse} = \frac{1}{10^S} \quad (2)$$

Where S is the final score from the vulnerability assessment using the rapid visual screening method.

Further details regarding the working procedure of the RVS method are illustrated in Figure 1:

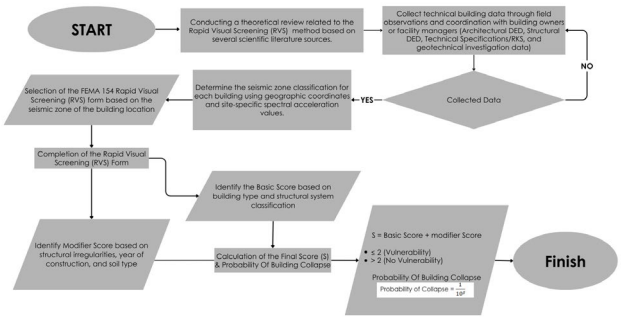


Figure 1 Procedure of The RVS Method

2.5 Inspection of vulnerable buildings using the demand capacity ratio (DCR)

The Demand Capacity Ratio (DCR) methodology is employed to quantify the necessary structural capacity and to identify structural elements that may be susceptible to failure. The DCR is determined using Equation (3) [30],[31].

$$DCR = \frac{Q_{UD}}{Q_{CE}} \quad (3)$$

If all DCR values calculated for a structural element are less than or equal to 1, then the element is anticipated to respond elastically to the seismic vibrations under analysis. Conversely, if the calculated DCR exceeds 1, the component is deemed to respond inelastically, suggesting the potential for permanent damage during an earthquake [32]. Table 1 explains the values of the demand capacity ratio and their safety levels [23],[33],[34].

Table 1 Demand Capacity Ratio Value [34]

Demand capacity ratio (DCR)	Safety Level
∞	Cover design
> 0 s/d 0.5	Safe
0.5 s/d 0.7	Safe
0.7 s/d 0.9	Safe
0.9 s/d 1.0	Fairly safe
>1.0	Over strength

To conduct further analysis using the demand capacity ratio method, the following steps are necessary.

Determining standards for evaluating the capacity of building structural elements ensures that the analysis is performed correctly and accurately. Establishing proper standards is crucial to ensure that all structural elements are thoroughly assessed and in line with applicable safety criteria [35].

DOI: https://doi.org/10.11113/jurnalteknologi.v88.25549

Modelling existing buildings in SAP2000 requires carefully considering all established design parameters and technical specifications to ensure the modelling results accurately reflect the building's actual conditions.

Loading and load combinations in SAP2000 are used at this stage to evaluate the structure's performance according to established standards [35].

The assessment of inter-story drift aims to identify the most vulnerable element of the structure in the event of a future seismic event. The inter-story drift observed within a building can be quantified employing the formula presented in Equation (4) [36].

This equation is used to determine the inter-story drift design value (δ_x) by multiplying the deflection amplification factor (C_d) with the elastic deflection (δ_{xe}) followed by normalization using the importance factor (I_e). The resulting inter-story drift represents the estimated actual structural deformation, taking into account the building importance level and the structural response under seismic loading.

$$\delta_x = \frac{C_d\, \delta_{xe}}{I_e} \tag{4}$$

After the inter-story drift results are obtained, those results are then compared with the allowable drift limits for each story using the calculation formula in Equation (5) [36].

This equation specifies that the maximum allowable inter-story drift (Δ_x) is limited to 0.020 of the story height (h_x). This limit is adopted to ensure that the structure does not experience excessive damage under seismic loading. The specified value also serves as an acceptance criterion to evaluate whether the previously calculated design drift remains within permissible safety limits.

$$\Delta_x = 0{,}020\,.\,h_x \tag{5}$$

If the analysis indicates that the permitted inter-story drift is less than the observed drift on one or more stories, that story should be considered critical. Such stories fail to meet the required inter-story drift standards and could be at risk of damage or collapse in a future earthquake [37].

Determining the value Q_{UD} of each structural element produces internal forces on the structural elements based on the analysis output of the building, using the SAP2000 software.

The calculation of Q_{CE} for each structural element requires determining its load-bearing capacity, which must be based on the specific structure used. If the building being reviewed is a reinforced concrete structure, the value of Q_{CE} can be determined and calculated based on SNI 2847:2019, which outlines the structural concrete requirements for building structures [38]. Meanwhile, if the building under review is a steel structure, the Q_{CE} value can be determined and calculated based on SNI 1729:2020, which outlines the requirements for structural steel buildings [39].

DCR Value Calculation, at this stage, calculations will be performed by comparing the values Q_{UD} and Q_{CE} of each element using the formula in equation (3). Further details regarding the working procedure of the DCR method are illustrated in Figure 2:

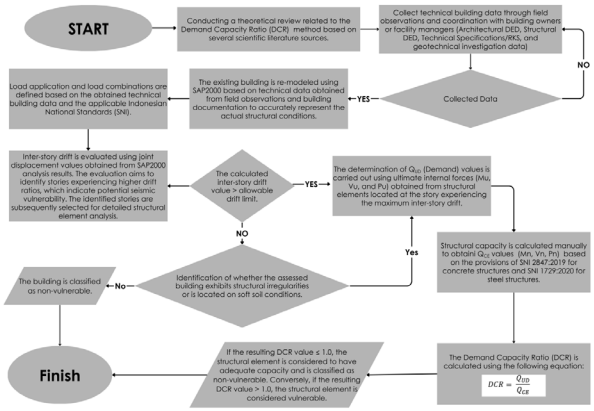


Figure 2 Procedure Of The DCR Method

2.6 Analysis of factors causing the vulnerability of existing buildings to earthquakes

A comprehensive analysis was performed to identify the factors contributing to the vulnerability of these buildings, using data from rapid visual screening and demand capacity ratio methods. After evaluating structural vulnerability with both approaches, the main factors identified from each method were compared to determine which were most influential in causing interconnected vulnerabilities.

To facilitate a clearer understanding of each stage of the research process, the research flowchart is presented in Figure 3.

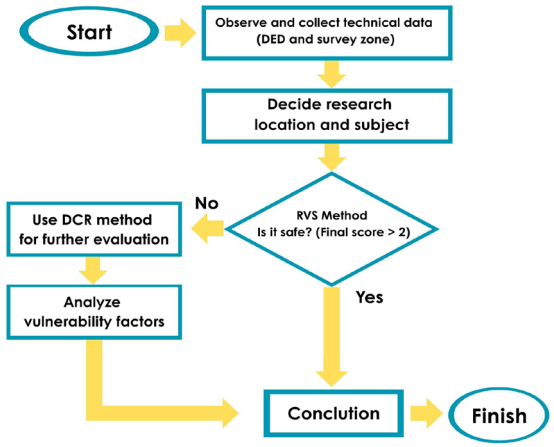


Figure 3 Research Flowchart

DOI: https://doi.org/10.11113/jurnalteknologi.v88.25549

3.0 RESULTS AND DISCUSSION

3.1 Results of assessment using the rapid visual screening (RVS) method

Before conducting a building vulnerability assessment with the RVS method, first determine the seismic zone for each building at the research site.

The seismic zone is determined by identifying the short-period spectral acceleration (S_S) and the long-period spectral acceleration (S_1) at the study site using the seismic design web-based application developed by the Ministry of Public Works and Housing (https://rsa.ciptakarya.pu.go.id/. Table 2 shows details on how seismic zones are identified [26].

Based on the analysis conducted on the seismicity zone of the building location, it was determined that each building studied was situated in a Moderately High seismicity zone; therefore, the FEMA 154 form that must be utilized is the Moderately High form [26].

Table 2 Seismicity Zone of the Research Location

Building	S_S	S_1	Seismicity zone
Public parking building	0.814	0.395	Moderately High
Public office building	0.817	0.397	Moderately High
Traditional market building	0.817	0.397	Moderately High
Public health building	0.798	0.386	Moderately High
SMEs Industrial building.	0.808	0.391	Moderately High

In FEMA 154, the basic score is determined by the building system and structure type, using technical data specific to each building [26]. Table 3 shows the basic scores for all the buildings examined.

Table 3 Building Basic Score

Building	Structure Type	Basic Score
Public parking building	S1	2.3
public office building	C1	1.7
traditional market building	C1	1.7
public health building	C1	1.7
SMEs Industrial building	S1	2.3

According to FEMA 154, the modifier score is closely related to the characteristics or parameters of building performance. If the building's characteristics improve performance, the modifier score is positive; if they decrease performance, it is negative [26]. Building performance parameters based on FEMA 154 include vertical irregularity, Plan Irregularity, year of construction, and the type of land on which the building was erected. Table 4 shows details of the modification score based on the building's performance parameters.

Table 4 Building Modifier Score

Building	Building performance parameters	Modifier Score
Public parking building	Weak and/or soft story	-1.1
	Post-benchmark	1.4
	Soil type (E)	-0.7
Public office building	Weak and/or soft story	-1.0
	Post-benchmark	1.9
Traditional market building	Sloping site	-0.6
	Short column	-1.0
	Non-parallel system	-0.7
	Post-benchmark	1.9
Public Health Building	Sloping site	-0.6
	Split level	-0.6
	Torsional	-0.7
	Post-benchmark	1.9
	Soil type (E)	-0.2
SMEs Industrial building	Sloping site	-0.7
	Split level	-0.7
	Reentrant corner	-0.9
	Post-benchmark	1.4

The final step in the RVS building vulnerability assessment involves determining the Final Score and the likelihood of the building collapsing. The Final Score is calculated using the FEMA 154 Rapid Visual Screening form and Equation (1), which is by adding the basic score with the modifier score that has been identified first, while Equation (2) is used to estimate the possibility of collapse that may occur in the event of a maximum earthquake so that later it can be known which buildings can be prioritized first for mitigation and further evaluation [26]. Table 5 and Figure 4 show the Final Score result, while Figure 5 shows the probability of collapse.

Table 5 Building Final Score

Building	Basic Score	Modifier Score	Final Score
Public parking building	2.3	-1.1 1.4 -0.7	1.9
Public office building	1.7	-1.0 1.9	2.6
Traditional market building	1.7	-0.6 -1.0 -0.7 1.9	1.3
Public health building	1.7	-0.6 -0.6 -0.7 1.9	1.5
SMEs Industrial building.	2.3	-0.2 -0.7 -0.7 -0.9 1.4	1.4

DOI: https://doi.org/10.11113/jurnalteknologi.v88.25549

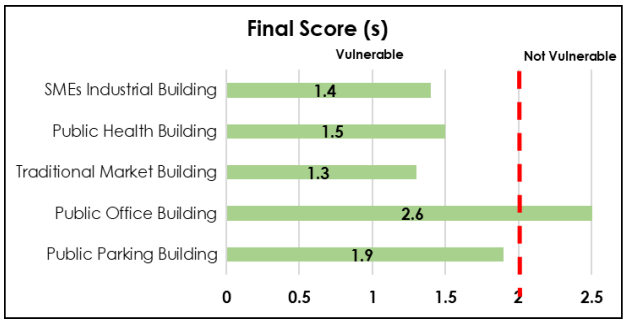


Figure 4 RVS Final Score

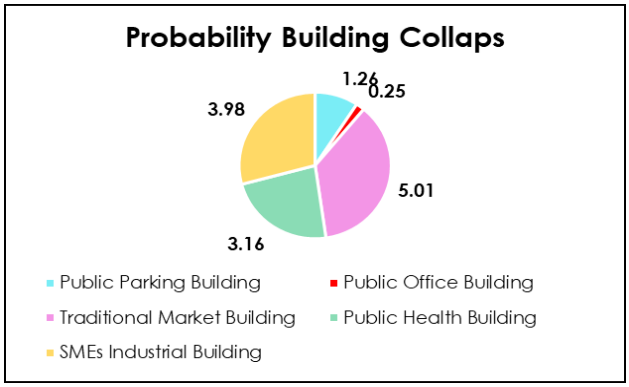


Figure 5 RVS Probability Value

The analysis indicates that Traditional Market buildings are most susceptible to earthquakes, as evidenced by the RVS methodology. Figure 5 demonstrates that these structures exhibit higher probability values compared to others. Nevertheless, since the final scores of several buildings are 2 or fewer, those buildings with such scores necessitate additional evaluation employing the DCR method.

3.2 Structural Evaluation Based on Demand Capacity Ratio (DCR)

To progress to the next phase of evaluation employing the DCR method, comprehensive technical data are indispensable. Accordingly, in this study, the advanced assessment was solely conducted on the public parking building, the traditional market building, and the public health building. For the SMEs industrial building, the technical data obtained remains insufficient to support further analysis using the DCR method [40]. The technical data for each building modeled in the follow-up evaluation using the DCR method are presented in Tables 6, 7, and 8.

Table 6 Technical Data of Public Parking Building

Structural Elements	Material	Dimensions (mm)	Grade (MPa)
Beam (B1)	Wide Flange steel	500 x 200 x 10 x 16	f_y = 240, f_u = 400
Beam (B2)	Wide Flange steel	400 x 200 x 8 x 13	f_y = 240, f_u = 400
Beam (B3)	Wide Flange steel	300 x 150 x 6.5 x 9	f_y = 240, f_u = 400
Beam (B4)	Wide Flange steel	250 x 125 x 6 x 9	f_y = 240, f_u = 400
Column (K1)	Steel HB	350 x 350 x 12 x 19	f_y = 240, f_u = 400
Column (K2)	Steel HB	250 x 250 x 9 x 14	f_y = 240, f_u = 400
Column (KP1)	Reinforced concrete	300 x 400	K300
Column (KP2)	Reinforced concrete	500 x 500	K300
Sloof (SL1)	Reinforced concrete	250 x 500	K300
Sloof (SL2)	Reinforced concrete	200 x 300	K300
Slab	Reinforced concrete	Thickness 120	K300

Table 7 Technical Data of Traditional Market Building

Structural Elements	Material	Dimensions (mm)	Grade (MPa)
Beam (B1)	Reinforced concrete	300 x 600	f'_c = 26,4
Beam (B2)	Reinforced concrete	300 x 400	f'_c = 26,4
Beam (B3)	Reinforced concrete	300 x 600	f'_c = 26,4
Beam (BA1)	Reinforced concrete	250 x 500	f'_c = 26,4
Beam (BK)	Reinforced concrete	300 x 500	f'_c = 26,4
Column (K1)	Reinforced concrete	500 x 500	f'_c = 26,4
Column (K2)	Reinforced concrete	400 x 400	f'_c = 26,4
Beam (RB1)	Reinforced concrete	300 x 400	f'_c = 26,4
Beam (RB2)	Reinforced concrete	300 x 400	f'_c = 26,4
Beam (RBA1)	Reinforced concrete	250 x 400	f'_c = 26,4
Slab (P1)	Reinforced concrete	Thickness 100	f'_c = 26,4
Slab (P2)	Reinforced concrete	Thickness 200	f'_c = 26,4
Slab (P3)	Reinforced concrete	Thickness120	f'_c = 26,4

Table 8 Technical Data of Public Health Building

Structural Elements	Material	Dimensions (mm)	Grade (MPa)
Beam (B1)	Reinforced concrete	300 x 400	f'_c = 25
Beam (B2)	Reinforced concrete	200 x 300	f'_c = 25
Beam (BK)	Reinforced	300 x 400	f'_c = 25

DOI: https://doi.org/10.11113/jurnalteknologi.v88.25549

Structural Elements	Material	Dimensions (mm)	Grade (MPa)
Beam (RB1)	concrete Reinforced concrete	300 x 400	f'_c = 25
Beam (RB2)	Reinforced concrete	200 x 300	f'_c = 25
Column(K1)	Reinforced concrete	300 x 500	f'_c = 25
Column (K2)	Reinforced concrete	300 x 500	f'_c = 25
Column (K3)	Reinforced concrete	300 x 300	f'_c = 25
Slab	Reinforced concrete	Thickness 120	f'_c = 25

This study focuses on the structural modeling of the building's main components, which support and distribute the primary loads. Figures 6, 7, and 8 illustrate the remodeling of the existing building structures.

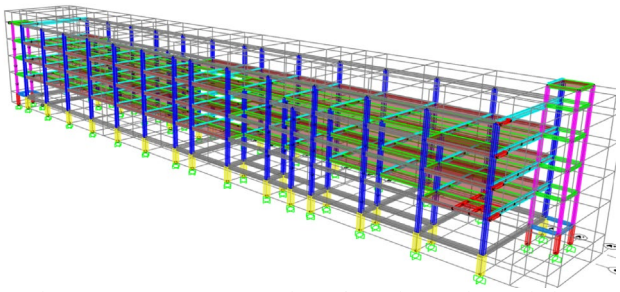


Figure 6 Structural Modelling of Public Parking Building

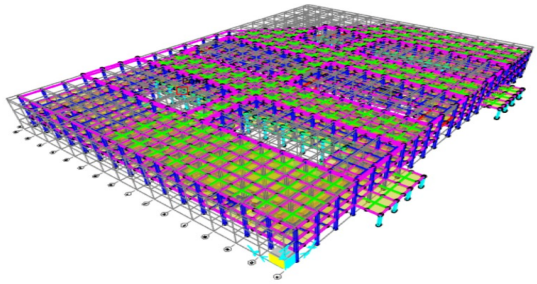


Figure 7 Structural Modelling of Traditional Market Building

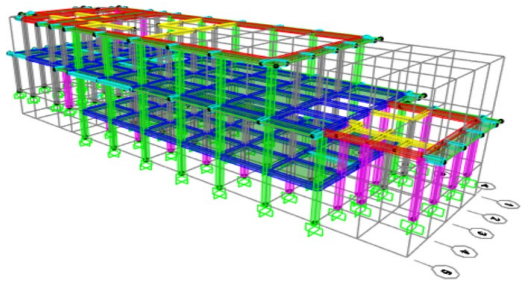


Figure 8 Structural Modelling of Public Health Building

Loads on the existing building are determined in accordance with SNI 1727:2020 regulations [41], which supersede the previous 2013 version. The updated rules are designed to ensure safety, durability, and alignment with current knowledge and technology. This study examines gravitational loads (including live, dead, and additional dead loads) and seismic loads. Wind, rain, and flood loads are excluded, as they generally have minimal impact on the main structure.

Following the loading of the building, a structural analysis is conducted by assessing the inter-story drift. The goal of evaluating inter-story drift is to determine which areas of the structure are most susceptible to future earthquakes. The formulas shown in Equations (4) and (5) can be used to determine the inter-story drift in a building [28],[36].

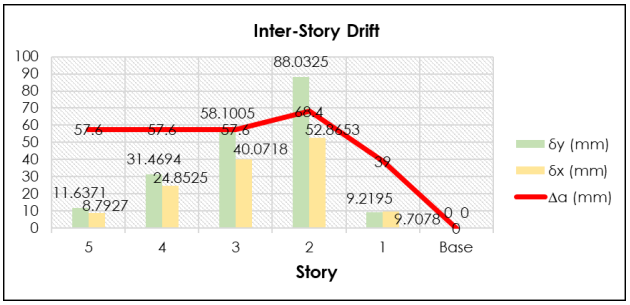


Figure 9 Inter-story Drift of Public Parking Building

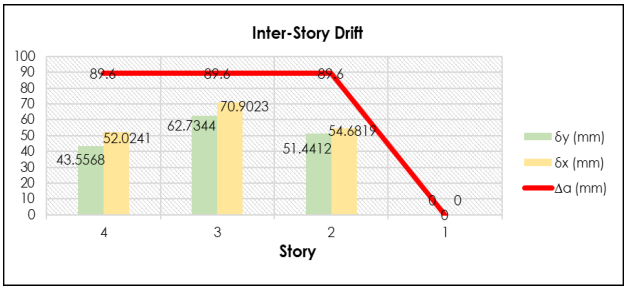


Figure 10 Inter-story Drift of Traditional Market Building

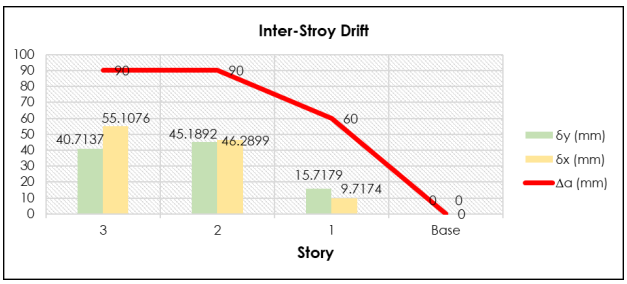


Figure 11 Inter-story Drift of Public Health Building

Following the calculation of inter-story drift values shown in Figures 9, 10, and 11, the analysis focuses on

DOI: https://doi.org/10.11113/jurnalteknologi.v88.25549

the maximum inter-story drift at the identified vulnerable story. If a vulnerable story is not explicitly specified, the study considers the story with the largest inter-story drift [42]. This method is supported by the initial Rapid Visual Screening (RVS) results, which identify structural irregularities within the building.

Once the maximum inter-story drift is identified, determine the Q_{UD} value for each structural element using SAP2000 software, which calculates Q_{UD} based on internal forces from applied loads [32].

The Q_{UD} value is the maximum internal force acting on the structure under the applied loading. The Q_{UD} value is taken from the Ultimate value of each internal force that occurs for each element of the structure, which in this case is the value of Mu, Vu, and Pu [42]. Tables 9 through 12 show the results for each main structural element.

Table 9 Q_{UD} Value of The Public Parking Building

Structural Element	Mu (kNm)	Vu (kN)	Pu (kN)
Beam (B1)	332.4519	169.917	53.6090
Beam (B2)	195.4436	141.0880	47.0247
Beam (B3)	166.7025	126.8250	62.8790
Beam (B4)	0.7051	1.373	8.283
Column (K1)	609.6502	203.1580	46.1290
Column (K2)	107.424	74.5240	159.104

Table 10 Q_{UD} Value of the Second-Story Traditional Market Building

Structural Element	Mu (kNm)	Vu (kN)	Pu (kN)
Beam (B1)	168.4487	179.5220	142.6700
Beam (B2)	74.8181	99.5730	106.7330
Beam (B3)	90.1139	67.3580	191.8870
Beam (BA1)	66.1947	56.3210	38.7590
Column (K1)	279.502	102.5390	0.0000
Column (K2)	145.9074	62.9560	265.3860

The inter-story drift analysis of the Public Health Building, shown in Figure 11, indicates that the maximum drift in the X and Y directions occurs on different stories. Therefore, each story with the maximum drift in either direction is evaluated separately [43].

Table 11 Q_{UD} Value of the Second-Story Public Health Building

Structural Element	Mu (kNm)	Vu (kN)	Pu (kN)
Beam (B1)	101. 5710	84.2860	132.7140
Beam (B2)	29.1586	33.3860	12.2290
Beam (RB1)	68.6588	49.9190	89.2020
Beam (RB2)	24.2304	17.4840	16.9060
Beam (BK)	1.0844	31.3030	33.6350
Column (K1)	78.4843	30.6670	0.0000
Column (K2)	229.4370	75.0790	25.1740
Column (K3)	81.8672	36.8720	19.0380

Table 12 Q_{UD} Value of the third-Story Public Health Building

Structural Element	Mu (kNm)	Vu (kN)	Pu (kN)
Beam (RB1)	68.1530	48.3590	41.0400
Beam (RB2)	24.6228	21.7960	23.0180
Beam (BK)	0.9704	41.9750	24.3170
Column (K1)	95.9901	39.0190	23.0180
Column (K2)	70.9794	27.7160	12.6260
Column (K3)	61.7097	25.5800	25.7890

Once the Q_{UD} values are determined for each building element, calculate the Q_{CE} value for each structural element. Use capacity analysis as specified in SNI 1729:2020 for steel structures and SNI 2847:2019 for reinforced concrete structures [39],[38].

The Q_{CE} value can be obtained by calculating the load capacity of each structural element. The Q_{CE} value is taken from the values Mn, Vn, and Pn, which are the standard parameters for the upper limit of the strength or capacity of a structural element in resisting deep force [44]. The Q_{CE} calculation results are displayed in Tables 13 through 16.

Table 13 Q_{CE} Value of The Public Parking Building

Structural Element	Mn (kNm)	Vn (kN)	Pn (kN)
Beam (B1)	458.40	720.00	2068.65
Beam (B2)	285.60	460.80	1529.46
Beam (B3)	115.44	846.32	846.32
Beam (B4)	77.76	216.00	679.97
Column (K1)	552.00	604.80	3182.13
Column (K2)	208.00	324.00	1679.94

Table 14 Q_{CE} Value of The Traditional Market Building

Structural Element	Mn (kNm)	Vn (kN)	Pn (kN)
Beam (B1)	241.0110	496.6576	4492.3468
Beam (B2)	145.2661	312.3691	3145.9468
Beam (B3)	382.7722	496.6576	4794.4447
Beam (BA1)	230.5808	386.6572	3368.3127
Column (K1)	677.2339	481.2045	7422.5874
Column (K2)	341.9857	341.9799	4798.7916

DOI: https://doi.org/10.11113/jurnalteknologi.v88.25549

Table 15 Q_{CE} Value of the Second-Story Public Health Building

Structural Element	Mn (kNm)	Vn (kN)	Pn (kN)
Beam (B1)	208.7456	286.6427	3281.4875
Beam (B2)	33.4090	135.0097	1421.7607
Beam (RB1)	158.6841	219.1876	3072.4911
Beam (RB2)	48.0447	134.1424	1497.3120
Beam (BK)	78.870 1	153.8624	2283.0200
Column (K1)	134.1146	285.5076	3500.9947
Column (K2)	134.1146	285.5076	3500.9947
Column (K2)	67.8025	152.8676	2225.9947

Table 16 Q_{CE} Value of The Third-Story Public Health Building

Structural Element	Mn (kNm)	Vn (kN)	Pn (kN)
Beam (RB1)	158.6841	219.1876	3072.4911
Beam (RB2)	48.0447	134.1424	1497.3120
Beam (BK)	78.8701	153.8624	2283.0200
Column (K1)	134.1146	285.5076	3500.9947
Column (K2)	134.1146	285.5076	3500.9947
Column (K3)	67.8025	152.8676	2225.9947

Once the Q_{UD} and Q_{CE} values are established, calculate the Demand Capacity Ratio (DCR) for each structural element using Equation (3) [32]. The resulting DCR values are shown in Figures 12, 15, 16, and 17.

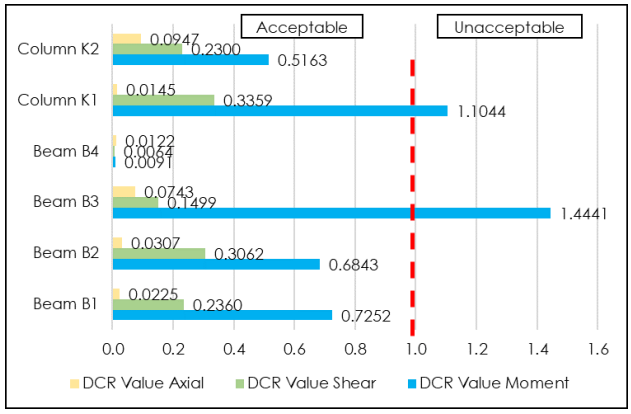


Figure 12 DCR Value of Public Parking Building

The Demand Capacity Ratio (DCR) analysis indicates that beam B3 and column K1 in the Public Parking Building, as illustrated in Figure 12, have DCR values exceeding 1 for moment forces. This confirms that their moment resistance is insufficient to resist the applied forces, raising the risk of damage or failure during seismic events. Figures 13 and 14 depict the locations of beam B3 and column K1.

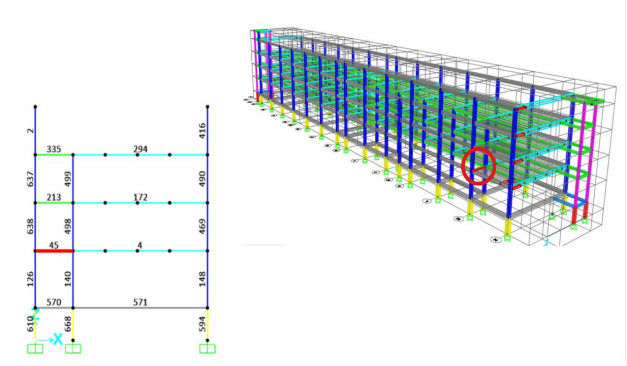


Figure 13 Critical Structural Element Beam B3

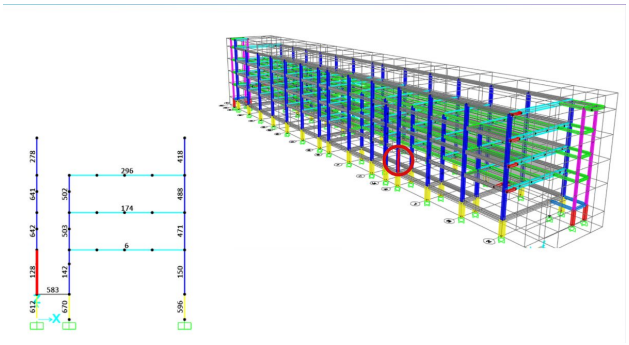


Figure 14 Critical Structural Element Column K1

The structural analysis of the Public Parking Building, using the Demand Capacity Ratio (DCR) method, shows that most elements are within safe limits (DCR ≤ 1). However, beam B3 and column K1 exceed the allowed DCR for moment forces, indicating insufficient capacity and a higher risk of earthquake damage. Column K1 is especially critical because it does not meet the strong column–weak beam requirement specified in SNI 1726:2019.

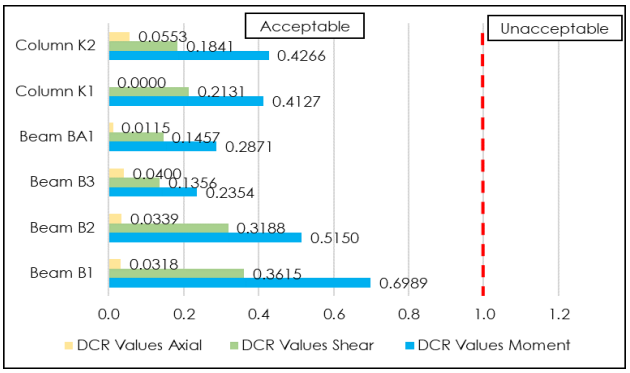


Figure 15 DCR Value of Traditional Market Building

Figure 15 shows that all the elements of the structure reviewed have a DCR value ≤ 1, this shows that the structural elements have a greater capacity to withstand loads than the internal forces acting on the

DOI: https://doi.org/10.11113/jurnalteknologi.v88.25549

structural elements, be it momentary, shear or axial forces. So it can be concluded that the Traditional Market building is in safe condition and meets the requirements for structural performance against earthquake loads. The building structure is estimated to be able to function properly without suffering significant damage in the event of an earthquake.

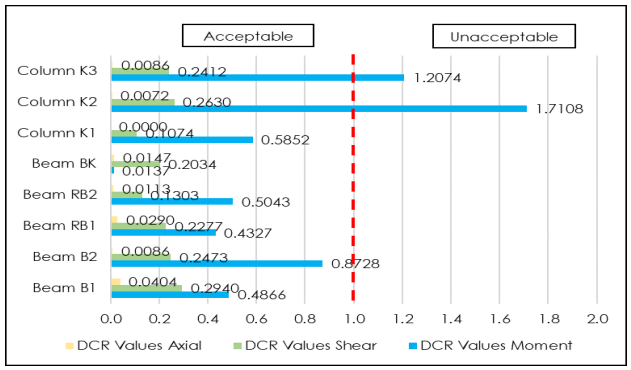


Figure 16 DCR Value of Second-Story Public Health Building

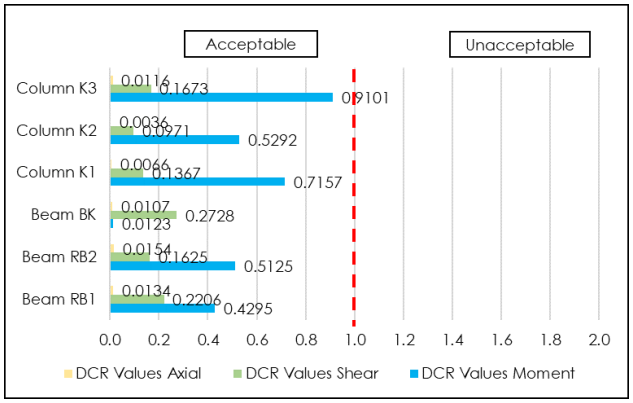


Figure 17 DCR Value of Third-Story Public Health Building

The DCR analysis for the second and third stories of the Public Health Building, shown in Figures 16 and 17, indicates that the third story is relatively safe, with all structural elements having DCR values of ≤ 1. On the second story, however, columns K2 and K3 have moment DCR values greater than 1, suggesting they lack sufficient capacity to resist moment forces and are at increased risk of damage or failure during an earthquake. Since the strong column–weak beam principle is not satisfied, these columns may fail before the beams, significantly increasing the risk of structural collapse. The locations of these columns are shown in Figures 18 and 19.

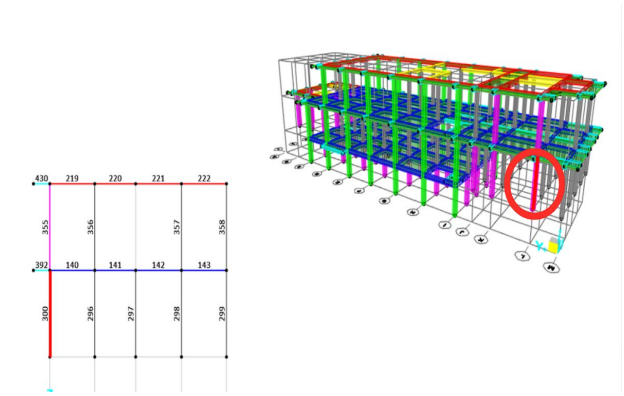


Figure 18 Critical Structural Element Column K2

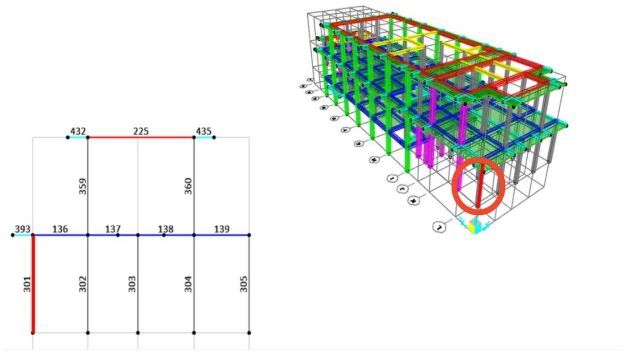


Figure 19 Critical Structural Element Column K3

3.3 Main Contributing Factors to Building Seismic Vulnerability

The determination of building vulnerability factors involved identifying parameters that exert the greatest influence on the assessment results of both the Rapid Visual Screening (RVS) and Demand Capacity Ratio (DCR) methods. Parameters that reduce the RVS score and simultaneously produce demand-to-capacity ratios exceeding the acceptable safety threshold were interpreted as contributing to increased structural vulnerability. The relationship between the two methods was evaluated by examining the consistency of assessment trends, where parameters that lead to a reduction in visual screening scores generally correspond to a decrease in the structural capacity to resist seismic loads.

Based on the results of Rapid Visual Screening (RVS) and Demand Capacity Ratio (DCR) analyses of low- to medium-rise buildings in Surakarta City, three main factors are identified as contributing to the buildings' vulnerability to earthquakes [26],[32].

The first factor is vertical structural irregularity. All buildings identified as vulnerable by the RVS had vertical irregularities; buildings with more than one type of irregularity were more vulnerable. The results

DOI: https://doi.org/10.11113/jurnalteknologi.v88.25549

of the DCR analysis also support this finding, especially in the Public Parking Building and Public Health Building, where some structural elements have DCR values greater than 1. This condition indicates that these elements lack sufficient capacity to withstand loads, primarily due to seismic moments [28].

The second factor is the type of soil the building is built on. Buildings on soft soil generally have lower final RVS scores than those on medium soil, indicating a higher risk of vulnerability. This is supported by DCR analysis, which shows DCR values exceeding 1 in the structural elements of buildings on soft soil, such as the Public Parking Building and the Public Health Building. This condition suggests that soft soil greatly increases the risk of structural failure during an earthquake [21].

The third factor influencing building vulnerability is the building standards or regulations applied during the planning phase. Structures that were not designed in accordance with the latest regulations, such as the Public Parking Building and the Public Health Building, exhibit elements with DCR values exceeding 1, making them more prone to structural failure under seismic loads. In contrast, the Traditional Market Building, although it appears vulnerable based on RVS, shows that all its elements stay safe (DCR ≤ 1). This is because the latest standards, specifically SNI 1729:2019, which are more rigorous in planning and more thoroughly consider safety factors, have been applied [40],[44].

4.0 CONCLUSION

According to the study's findings, four of the five buildings examined using the Rapid Visual Screening (RVS) method, the public parking structure, the traditional market structure, the public health center building, and the SMEs industrial building, were classified as vulnerable, as their final scores were below 2. Additionally, the Public Parking Building and the Public Health Building have DCR values greater than 1, as determined through an additional evaluation using the Demand Capacity Ratio (DCR) method. This means that certain structural elements have moment forces that exceed their capacity, and therefore do not adhere to the strong column-weak beam principle outlined in SNI 1726:2019. The primary factors contributing to the seismic vulnerability of these buildings are structural irregularities, the soil type at the building site, and the design standards used during construction.

This study has introduced a linear, systematic procedure for assessing the seismic vulnerability of existing buildings by integrating Rapid Visual Screening (RVS) with Demand Capacity Ratio (DCR) analysis. The proposed framework combines rapid visual evaluation and structural capacity verification into a single assessment process, enabling a more reliable and consistent evaluation than applying each method independently. Beyond assessment, the framework's results can serve as a technical reference for identifying vulnerable structural elements and prioritizing appropriate retrofitting measures to mitigate seismic risk.

Furthermore, the proposed approach may support government agencies and decision-makers in formulating evidence-based mitigation strategies, particularly in determining intervention priorities for existing buildings in earthquake-prone areas. However, the framework is limited to linear analysis and does not explicitly represent nonlinear structural behavior or collapse mechanisms under extreme seismic demands, which remain subjects for further investigation.

Acknowledgement

This research received full funding from the Directorate of Research and Community Service under the Master's Thesis Research Scheme, 127/C3/DT.04.00/PL/2025. The authors acknowledge the Directorate of Research and Community Service (DPPM) and the Ministry of Higher Education for providing the financial support necessary to conduct this study.

Conflicts of Interest

The authors declare that there is no conflict of interest regarding the publication of this paper.

Data availability

The data supporting the findings of this study are available from the corresponding author upon reasonable request.

Ethics declaration

Formal ethical approval was not obtained for this study. However, the authors confirm that the research was conducted in accordance with established ethical principles and good research practices, with due consideration given to participant rights, informed consent, confidentiality, and responsible data handling.

References

[1] R. J. Geller, "Earthquake prediction: a critical review," *Geophys. J. Int.*, Vol. 131, No. 3, pp. 425–450, 1997, DOI: https://10.1111/j.1365-246x.1997.tb06588.x.

[2] N. B. Jarah, A. H. Hassin Alasadi, and K. M. Hashim, "Earthquake prediction technique: a comparative study," *IAES Int. J. Artif. Intell.*, Vol. 12, No. 3, pp. 1026–1032, 2023,

DOI: https://10.11591/ijai.v12.i3.pp1026-1032.
[3] A. Ismail-Zadeh, "Earthquakes yes, disasters no," *npj Nat. Hazards*, Vol. 1, No. 1, 2024, DOI: https://10.1038/s44304-024-00049-0.
[4] I. A. Frege *et al.*, *World Risk Report 2023*. Berlin: worldRiskReport 2023, 2023. [Online]. Available: https://weltrisikobericht.de/wp-content/uploads/2024/01/WorldRiskReport_2023_english_online.pdf
[5] Verstappen, "Indonesian Landforms and Plate Tectonics," *J. Geol. Indones.*, Vol. 5, No. 3, pp. 197–207, 2010, doi: https://doi.org/10.17014/ijog.v5i3.103.
[6] N. Haris, A. C. Furqan, A. Kahar, and F. Karim, "Disaster risk index on disaster management budgeting: Indonesia's national data set," *Jamba J. Disaster Risk Stud.*, Vol. 15, No. 1, pp. 1–7, 2023, DOI: 10.4102/jamba.v15i1.1365.
[7] S. D. Rahmawati, "Spatial Modeling of Earthquake Risk in Sulawesi and Maluku Based on Geological Factors," Vol. 6, No. 2, pp. 235–247, 2025, DOI: 10.20956/ejsa.v6i2.45160.
[8] A. R. Bramantya, Sugiharto, and L. Mulya, "Documenting disaster in Yogyakarta: A case study of earthquake on May 27th, 2006," *Rec. Libr. J.*, Vol. 10, No. 2, pp. 247–260, 2024, DOI: 10.20473/rlj.V10-I2.2024.247-260.
[9] Maidiawati, J. Tanjung, Y. Sanada, F. Nugroho, and S. Wardi, "Seismic analysis of damaged buildings based on post-earthquake investigation of the 2018 Palu earthquake," *Int. J. GEOMATE*, Vol. 18, No. 70, pp. 116–122, 2020, DOI: 10.21660/2020.70.9490.
[10] A. Fajar, N. Sarjan, and I. H. Muchtaranda, "Review of the 2018 Lombok Earthquake, Indonesia, and Its Impact from Previous Studies," *Proc. First Mandalika Int. Multi-Conference Sci. Eng. 2022, MIMSE 2022 (Civil Archit.*, pp. 76–84, 2023, DOI: 10.2991/978-94-6463-088-6.
[11] S. Pratiwi, "Determination of Earthquake Vulnerability Level Using the Microtremor Refraction (ReMi) Method in Surakarta City (Penentuan Tingkat Kerawanan Gempa Bumi Menggunakan Metode Refraksi Mikrotremor (ReMi) di Kota Surakarta)," *Indones. J. Appl. Phys.*, Vol. 7, No. 1, p. 58, 2017, DOI: 10.13057/ijap.v7i1.4884.
[12] Y. M. Purwana M.T., R. H. Dananjaya, and Y. C. Nogroho, "Updating of Surakarta Seismic Site Class Map Based on Standard Penetration Test," *J. Ris. Rekayasa Sipil*, Vol. 3, No. 2, p. 84, 2020, DOI: 10.20961/jrrs.v3i2.41085.
[13] Tim Detik Jogja, "A magnitude 5.2 earthquake shook the waters of Gunungkidul (Gempa M 5,2 Goyang Perairan Gunungkidul)," Yogyakarta, 2026. [Online]. Available: https://www.detik.com/jogja/berita/d-7758146/gempa-m-5-2-goyang-perairan-gunungkidul
[14] Badan Pusat Statistik Provinsi Jawa Tengah, "Population by Regency/City in Central Java, 2023 (Jumlah Penduduk Menurut Kabupaten/Kota di Jawa Tengah, 2023)," 2023. [Online]. Available: https://jateng.bps.go.id/id/statistics-table/2/NzY2IzI=/jumlah-penduduk-menurut-kabupaten-kota-di-jawa-tengah.html
[15] L. B. Grant, "Paleoseismology," in *International Handbook Of Earthquake and Engineering Seismology*, California, 2002, pp. 475–489. DOI: https://doi.org/10.1016/S0074-6142(02)80233-9.
[16] P. Mahto and S. C. Gupta, "Tectonic stress regime and faulting style analysis due to sequence of earthquakes in Western Nepal," *Nat. Hazards Res.*, Vol. 4, No. 4, pp. 531–538, 2024, DOI: 10.1016/j.nhres.2023.11.010.
[17] P. Bountzis, C. Kouroukla, P. Bonatis, V. Karakostas, E. Papadimitriou, and A. Kostoglou, "Triggering mechanisms and repeating earthquakes during the intense 2020-2021 seismic crisis in the Gulf of Corinth," *Geophys. J. Int.*, Vol. 242, No. 2, pp. 1–18, 2025, DOI: 10.1093/gji/ggaf181.
[18] M. Ujianto, A. Z. M. Ali, and M. Solikin, "Structural Behavior of Precast Concrete Wall Panels Due," Vol. 050013, No. July, 2023.
[19] Z. Yilmaz *et al.*, "Regional Building Damage Survey Data on the 2023 Kahramanmaraş, Türkiye, Earthquakes," *ASCE OPEN Multidiscip. J. Civ. Eng.*, Vol. 2, No. 1, pp. 1–25, 2024, DOI: 10.1061/aomjah.aoeng-0041.
[20] S. Li, Y. Zhang, Z. Du, C. Zhai, and L. Xie, "Quantitative evaluation on building collapse-induced human casualty for performance-based earthquake engineering," *Sustain. Dev. Crit. Infrastruct. - Proc. 2014 Int. Conf. Sustain. Dev. Crit. Infrastruct.*, No. December, pp. 197–203, 2014, DOI: 10.1061/9780784413470.019.
[21] Siddharth and A. K. Sinha, "Rapid visual screening vulnerability assessment method of buildings: a review," *Int. J. Adv. Technol. Eng. Explor.*, Vol. 9, No. 88, pp. 326–336, 2022, DOI: 10.19101/IJATEE.2021.874605.
[22] V. N. Wankhade, "A Seismic Vulnerability and Fragility of RC Conventional and Monolithic Building," *Int. J. Res. Appl. Sci. Eng. Technol.*, Vol. 10, No. 6, pp. 4732–4743, 2022, DOI: 10.22214/ijraset.2022.45042.
[23] FEMA 310, *Handbook for the Seismic Evaluation of Buildings: A Prestandard*. Washingtong D.C, 1998. [Online]. Available: https://mitigation.eeri.org/wp-content/uploads/fema310.pdf
[24] E. Juliafad and H. Gokon, "Seismic Fragility Function For Single Storey Masonry Wall Rc Building In Padang City , Indonesia," Vol. 22, No. 94, pp. 39–46, 2022, DOI: https://doi.org/10.21660/2022.94.3160.
[25] A. Yeşilyurt, "Seismic vulnerability and risk assessment of a typical RC school building using hybrid-based fragility curves," Vol. 5, No. 2, pp. 796–811, 2025, DOI: https://doi.org/10.61112/jiens.1679569.
[26] FEMA-154, *Rapid visual screening of buildings for potential seismic hazards: FEMA 154 and FEMA 155 updates*, No. January. Washington D.C, 2015. DOI: https://doi.org/10.1061/9780784479728.064.
[27] M. A. Rofiq, M. Tsabit, and R. Bachtiar, "High Quality Reinforced Due To Axial Loading (Bertulang Mutu Tinggi Akibat Beban Aksial)," *Pros. Simp. Nas. Rekayasa Apl. Peranc. dan Ind.*, pp. 104–106, 2020.
[28] N. Hassan, S. R. Chowdhury, and R. I. Shuvo, "Seismic Behavior Of Multi-Storied RC Building With Re-Entrant Corner," *J. Teknol.*, Vol. 2, pp. 183–198, 2024, DOI: 10.11113/jurnalteknologi.v86.20656.
[29] N. Ramly, M. Alel, A. Adnan, and E. T. Mohamad, "A Simplified Method for Preliminary Seismic Vulnerability Assessment of Existing Buildings in Kundasang, Sabah, Malaysia," *J. Teknol.*, Vol. 3, pp. 1–7, 2015, DOI: 10.11113/jt.v72.4003.
[30] R. S. Siregar, Z. Djauhari, and Ridwan, "The Effect of Site Class Classification According to SNI 1726-2019 on Progressive Collapse of Irregular Building Structures (Pengaruh Klasifikasi Kelas Situs Menurut SNI 1726-2019 Terhadap Keruntuhan Progresif pada Struktur Gedung Tidak Beraturan)," *Sainstek (e-Journal)*, Vol. 9, No. 2, pp. 123–131, 2021, DOI: 10.35583/js.v9i2.153.
[31] N. K. Handayani, "Evaluation of Structural Performance of Existing Building Seven-Story Building with FEMA 310 (Evaluasi Kinerja Struktur pada Gedung Eksisting Tujuh Lantai dengan FEMA 310)," *J. Tek. Sipil dan Teknol. Konstr.*, Vol. 7, No. 1, pp. 1–14, 2021, DOI: https://doi.org/10.62603/konteks.v2i1.241.
[32] FEMA 356, *Prestandard and Commentary for the Seismic Rehabilitation of Buildings - FEMA 356*, No. November. Washington D.C, 2000. [Online]. Available: https://www.nehrp.gov/pdf/fema356.pdf
[33] J. H. Sohn, I. S. Choi, and J. H. Kim, "Seismic Performance Evaluation by Demand Capacity Ratio in Vertical Irregular Buildings," in *The 17th World Conference on Earthquake Engineering*, 2020, No. September, pp. 1–12. [Online]. Available: https://www.researchgate.net/publication/360104051_Seismic_performance_evaluation_by_demand_capacity_ratio_in_vertical_irregular_buildings
[34] Y. Nurchasanah, A. Rochman, M. Ujianto, A. S. Fauzi, and A. H. Nugraha, "Assessments of the Vulnerability and Demand Capacity Ratio of Old Public Buildings Structures," *E3S Web Conf.*, Vol. 517, p. 7, 2024, DOI:

10.1051/e3sconf/202451705009.

[35] A. Febrianto, Erizal, and H. Putra, "Seismic Analysis of Building Structures Using ASCE 41-17 and SNI 1726:2019 (Analisis Seismik Struktur Bangunan menggunakan ASCE 41- 17 dan SNI 1726 : 2019)," *Tek. Sipil dan Lingkung.*, Vol. 09, No. 02, pp. 211–220, 2024, DOI: 10.29244/jsil.9.2.211-220.

[36] SNI 1726, "Code of Practice for Earthquake-Resistant Design of Building and Non-Building Structures (Tata cara perencanaan ketahanan gempa untuk struktur bangunan gedung dan nongedung)," Badan Standarisasi Nasional, Jakarta, 2019. [Online]. Available: https://ciptakarya.pu.go.id/admin/assets/upload/galeri/gempa/2025/05/21/201747_1. SNI_1726_2019_Tata cara perencanaan ketahanan gempa untuk struktur bangunan gedung dan non gedung.pdf

[37] F. A. Nugroho, Y. Nurchasanah, and M. G. Fauzi, "Evaluation of Building Structural Performance Using Design Earthquake Response Spectrum Analysis Based on SNI 1726:2019 (Evaluasi Kinerja Struktur Gedung Menggunakan Analisis Respons Spektrum Gempa Desain SNI 1726:2019)," in *Prosiding Seminar Nasional Teknik Sipil 2024*, 2024, pp. 50–54. [Online]. Available: https://proceedings.ums.ac.id/sipil/article/view/3946/3597

[38] SNI 2847, "Requirements for Structural Concrete for Buildings (Persyaratan Beton Struktural untuk Bangunan Gedung)," Jakarta, 2019. [Online]. Available: https://tekonsipil.sv.ugm.ac.id/file/sni-2847-2019-persyaratan-beton-struktural-untuk-bangunan-gedung-sni-1726-2019-persyaratan-beton-struktural-untuk-bangunan-gedung/

[39] SNI 1729, "Specifications for Structural Steel Buildings (Spesifikasi untuk bangunan gedung baja struktural)," Jakarta, 2020. [Online]. Available: https://spada.uns.ac.id/pluginfile.php/650679/mod_resource/content/4/SNI 1729-2020 Spesifikasi untuk bangunan gedung baja struktural.pdf

[40] N. K. Handayani, B. M. Abadi, and N. D. Pamungkas, "Structural Performance Evaluation Of 7-Storey 1-Basement Hospital Building In Semarang By Linear Dynamic Analysis Of Variational Response And Time History Using The Reference Of Sni 1726:2019 (Evaluasi Kinerja Struktur Gedung Rumah Sakit 7 Lantai 1 Baseme," *J. Civ. Eng. Infrastruct. Technol.*, Vol. 3, No. 2, pp. 39–48, 2024, DOI: 10.36728/jceit.v3i2.4347.

[41] SNI 1727, "Minimum design loads and related criteria for buildings and other structures (Beban desain minimum dan Kriteria terkait untuk bangunan gedung dan struktur lain)," Jakarta, 2020. [Online]. Available: https://ciptakarya.pu.go.id/admin/assets/upload/galeri/gempa/2025/05/21/380575_3. SNI_1727_2020_Beban desain minimum dan kriteria terkait untuk bangunan gedung dan struktur lain.pdf

[42] F. Sun and B. Xiao, "Analysis on interstory drift of high-rise residential quasi-megastructure," *Adv. Struct. Eng.*, pp. 1–14, 2019, DOI: 10.1177/1369433218822091.

[43] Y. C. Assidiq and I. Bali, "Study of Base Shear and Inter-Story Drift due to Earthquake Forces on a Ten-Story Building Structure in Surakarta," Vol. 62, No. April, pp. 1–11, 2025, DOI: 10.33021/pcej.v3i1.5627.

[44] J.-W. Pang, C.-C. Yip, L. Ling, J. Y. Wong, F. S. Lam, and C. F. Wong, "Finite Element Simulation Of Low-Rise School Building Model With Seismic Loads Input," *J. Teknol.*, Vol. 6, pp. 141–152, 2024, DOI: 10.11113/jurnalteknologi.v86.22019|.